



**NTNU – Trondheim**  
Norwegian University of  
Science and Technology

# Parameter study of electric power production in wind farms - experiments using two model scale wind turbines

**Guro Tjomlid Maal**

Master of Energy and Environmental Engineering

Submission date: December 2014

Supervisor: Lars Sætran, EPT

Norwegian University of Science and Technology  
Department of Energy and Process Engineering



# Parameter study of two in-line model wind turbines in a shear flow

Guro Tjomlid Maal

Norwegian University of Science and Technology NTNU, 2014

## Abstract

A parameter study investigating the effects of adjusting tip speed ratios (TSR) and turbine distance in a model scale wind farm was conducted in the wind tunnel facility at NTNU. The aim was to identify optimal turbine operation and wind park design of the two model scale wind turbines when the downstream turbine operates in the wake of the upstream turbine. Experiments were conducted with turbine distances of 3.2, 5.3 and 9.0 diameters, and the power coefficient ( $C_p$ ) and thrust coefficient ( $C_t$ ) were mapped with TSR steps of 0.5. A shear generating grid was constructed to imitate typical offshore wind conditions with turbulence and shear. The experimental study revealed significant positive effects in  $C_p$  as well as a moderate increase in thrust when increasing the distance between the turbines. Both turbines had optimal tip speed ratios of 6 in an undisturbed flow, but the optimal TSR of the downstream turbine was found to be 4, 4.5 and 5 in varying turbine distances from 3.2 to 9.0, respectively. The optimal tip speed ratio of turbine 1 seemed to be slightly shifted towards a TSR of 5.5, but this shift was only present at the two smallest turbine distances. With these distances, the increased energy extraction of turbine two was larger than the energy loss of operating turbine 1 at a lower tip speed ratio than the design value. All turbine performance measurements conducted in a shear flow were also compared to similar measurements conducted in uniform flows with and without turbulence. The comparison revealed that turbulence has a significant positive effect on the efficiency on a downstream turbine, whereas the wind shear was found not to have any noticeable effect on the turbine performance.

## 1 INTRODUCTION

The technology of utilizing wind energy is thousands of years old, but significant aerodynamical improvements of wind turbines have been developed during the last decades. Since the 1970's, the aerodynamical efficiency of a wind turbine has increased from 0.4 to 0.5, i.e. enhancing the energy production by 25 % [14]. However, the potential of making wind energy more profitable may no longer be dependent on improving single turbine efficiency. An important focus in ongoing and future research is studying how multiple turbines interact in large wind farms, and how wind farms can be designed and operated with respect to this. Offshore wind farms, such as Horns Rev and Sheringham Shoal, are designed with a turbine spacing of around 7 diameters. Computational, wind tunnel and full scale studies have shown that this gives a total farm efficiency loss of between 5 and 15 %, depending on the wind conditions [1, 2, 11]. Wind tunnel measurements conducted at NTNU showed that operating the upstream turbine in yawed position can reduce the wake losses significantly [8]. It is therefore of interest to study how optimizing the position, rotational speed, yaw angle and pitch angle of turbines can reduce wake losses in a wind farm.

As there are few possibilities of doing experimental measurements on full scale wind farms, it is essential to produce realistic results from wind tunnel experiments

with controlled conditions and computational simulation models. A group at the Department of Energy and Process Engineering at NTNU has conducted three blind tests in NTNU's largest wind tunnel. The measurements mapped turbine performance and wake development for model wind turbines in varying tunnel setups [9, 10, 12]. Model simulation specialists from both Norwegian and international research communities made predictions of the results using a range of simulation methods. A significant potential of improving the accuracy and reliability of these methods was revealed, and it was decided to conduct a fourth blind test with a slight increase of flow complexity. The current study is a part of the collection of measurements which makes Blind test 4.

The aim of this study is two-fold. One focus will be on examining how changes in distance and rotational speed of two in-line model turbines affect the turbine efficiencies in a turbulent shear flow. The shear flow will be generated by a grid designed specifically for this study, and will imitate realistic wind conditions in a typical offshore atmospheric boundary layer. Secondly, the results will be compared to similar measurements conducted in a uniform flow, to investigate any changes in turbine performance due to wind shear. Hence, this research can reveal coherence between experimental and computational modelling results in Blind test 4, as well as contribute to optimizing wind farm design and operation.

## 2 EXPERIMENTAL METHODOLOGY

### Wind tunnel setup

The wind tunnel (Figure 1) is located in the Fluid Mechanics Building at NTNU, and is driven by an electrical fan which can generate wind with a velocity of up to 100 km/h. The experimental test section in the tunnel has a width of 2.7 m, a height of 1.8 m and a length of 11 m. Two wind turbine models with rotor diameters of 0.944 m and 0.894 m were positioned in a straight line in the centre of the tunnel. The turbine with the largest rotor diameter, hereby referred to as turbine 1 (T1), was positioned upstream. Hence, turbine 2 (T2) was positioned in the wake of turbine 1. Both turbines had a hub height of 830 mm above the tunnel floor. The rotor area is approximately 14 % of the cross sectional area of the tunnel, which is slightly higher than the recommended maximum of 10 percent [8]. Figure 2 shows a sketch of the setup, where the diameter of T2 is used as reference for the different distances. Measuring thrust force on the downstream turbine required it to be mounted on a 6 component balance. Hence, the respective turbine positions in which the forces could be measured was restricted to the positions of the hatches in the tunnel floor. It was therefore possible to conduct measurements with turbine spacings of 3.2, 5.3 and 9.0 diameters, whereas T1 was fixed at 2.0 diameters behind the tunnel inlet in all measurements.

The model turbines were designed in 2008, using the 14 percent thick NREL S826 airfoil along the whole span. The design was optimized for turbine 2, but was also used for turbine 1, which has slightly larger hub size. This may influence the efficiency of the turbine, as the blades are more sensitive to stall close to the hub. The turbines were designed with an optimal tip speed ratio of  $TSR = 6$ , meaning that a tunnel wind speed of 11,5 m/s would produce a Reynolds number,  $Re = \frac{c\omega R}{\nu}$ , of just over  $10^5$  ( $c$ =chord length at tip,  $\omega$ =rotational speed and  $\nu$ =kinematic viscosity). An estimation of a typical 2 MW

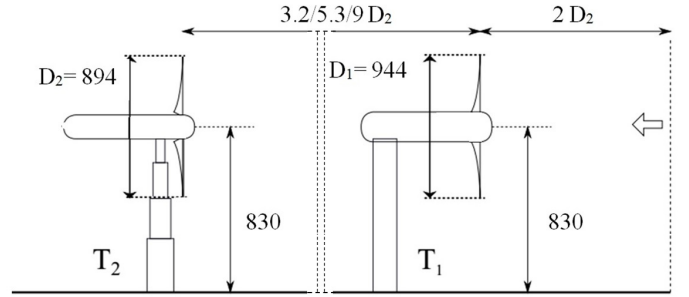


Figure 2: Sketch with dimensions [mm]

wind turbine would give a rotor diameter approximately 100 times larger than the model diameter. This means that in a full scale environment, the Reynolds number of this turbine would be 100 times larger, i.e. around  $10^7$ . Detailed information about the turbine characteristics and performance is described in Krogstad and Lund [8]

### Grid generated turbulence and shear

An essential part of this study was to create realistic offshore wind conditions for the experiments. It is possible to imitate three key characteristics of atmospheric wind in the wind tunnel; turbulence, wind speed and shear. As wind shear and turbulence is generated only at the grid position, their development throughout the tunnel was measured in all four turbine positions.

Wind shear is the vertical and horizontal difference in wind speed and direction. The thickness of the atmospheric boundary layer is hence equal to the height in which the wind shear due to surface properties is negligible. There are several approaches to describing atmospheric wind shear, but the power law is one of the most common. This law expresses the wind speed,  $U$ , as function of height,  $z$ , provided that the wind speed at an arbitrary reference height,  $z_r$ , is known:

$$\frac{U(z)}{U(z_r)} = \left(\frac{z}{z_r}\right)^\alpha \quad (1)$$

The power law coefficient,  $\alpha$ , describes the strength of shear in the wind profile, and hence varies strongly with the atmospheric stability and wind speed, the surface roughness and the terrain shape. The International Electrotechnical Commission (IEC) has published an international standard suggesting a velocity-independent offshore power law coefficient of 0.14 [4]. However, several measurements show that this coefficient often is slightly lower, and also strongly dependent on wind speed and atmospheric stability [6]. The FINO1 research platform in the North Sea measured a coefficient of 0.11 at a wind speed of 11 m/s [6]. Measurements conducted in stable atmospheric conditions in the Gulf of Mexico also gave a power law coefficient of  $0.11 \pm 0.03$  [7]. A wind profile based on a coefficient of 0.11 was therefore chosen as a reference for this study, and the shear generating grid was



Figure 1: The wind tunnel

Bar no. (from top)	Height [mm]
1	1600
2	1300
3	1015
4	795
5	575
6	385
7	203
8	40

Table 1: Positions of the horizontal bars in the shear generating grid, measured in the bar center.

designed to imitate this specific wind profile.

Turbulence is a measure of wind speed variations in time. It is often expressed in turbulence intensity, which is the standard deviation of the instantaneous wind speed divided by the average wind speed. The FINO1 measurements resulted in a typical turbulence intensity of around 5 % at a wind speed around 12 m/s, measured at 90 m height [6]. Doppler sodar measurements, conducted between 50 and 300 m height at the southern coast of Japan, gave a stable turbulence of just over 7 % at all heights [13], whereas the IEC standard suggests an average of 12 % for wind speeds around 15 m/s, and at 90 m height [3]. During the design process of the grid used in the current experiments, the turbulence was not a design criteria, but simply a result of the shear generating design. The final design of the bi-planar grid is shown in Figure 3 (a), and the horizontal bar positions in Table 1. The vertical bars have spaces of 240 mm.

#### *Procedure and elements of uncertainty*

Each separate measurement was finished in one day to avoid sudden changes in atmospheric air pressure. The wind speed was found by measuring static pressure difference in a contraction area in front of the tunnel test section. Pitot measurements of the shear flow in an empty

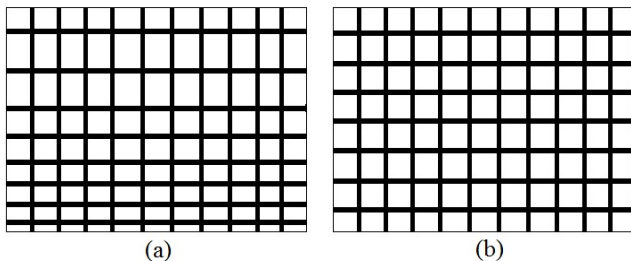


Figure 3: (a) The grid generating shear and turbulence. The mesh width is 240 mm, mesh heights vary between 16.5 (at floor) and 300 mm, and the solidity is 38 %. (b) The quadratic grid generating turbulence, with a mesh size  $M=240$  mm and solidity of 35 %. Both grids are bi-planar, and have quadratic bars with sides of 47 mm.

wind tunnel had shown that the velocity in hub height changed throughout the tunnel. Relation factors between contraction measurements and pitot measurements were therefore identified in each turbine position. These relation factors were used in further calculations to ensure the correct reference velocity in each turbine position. Both the static pressure difference and pitot velocity measurements were calibrated using a manually handled manometer, which could potentially be misread by  $\pm 0.5$  mm. A misreading of 1 mm showed to change the velocity by only 0.4 % and the turbine efficiency of 1.5 %. The tunnel fan was continuously adjusted so that the velocity was  $11.5 \pm 0.05$  m/s.

The turbulence intensity was measured using hot wire anemometry, calibrated with a pitot tube measurement. The hot wire had shown to have some drift in the signal, and was therefore calibrated before and after each measurement. It was never used for more than an hour between calibrations. In all hot wire measurements, the highest drift that was measured affected the turbulence intensity by 2,6 %.

Torque and RPM were measured inside the turbine nacelle, using a torque transducer and laser counter, respectively, and thrust was measured using a Schenck balance.

#### *Comparison of data*

The aim of this study was not only to examine the effects of turbine spacing and rotational speed in a shear flow, but also to see if the shear flow generated different results than a uniform flow did in previous measurements. The comparison measurements had partly been conducted using a turbulence generating bi-planar grid, shown in Figure 3 (b). This grid is designed to make a turbulent and uniform free stream, and is reviewed in Davidsen & Krogstad [5] and in the Blind test 3 paper [10]. It had shown to generate a turbulence of approximately 10% 2 diameters from the grid, which had dropped to 5% at 5 diameters from the grid. In a tunnel without grids, the flow has a low and constant turbulence intensity of 0.23%. Turbine distances of 2.8, 5.2 and 9.0 were examined in the comparison measurements.

When processing the results from this experiment and the comparison experiments, the main focus was on the power coefficient,  $C_P$ , and thrust coefficient,  $C_T$ , of turbine 1 and 2. Both coefficients are dimensionless functions of air density, rotor area and a reference velocity.  $C_P$  also requires a measurement of the power production,  $P_{rotor}$ , whereas  $C_T$  requires a measurement of the thrust force on the rotor,  $T_{rotor}$ :

$$C_P = \frac{P_{rotor}}{\frac{1}{2}\rho V_{ref}^3 A_{rotor}} \quad (2)$$

$$C_T = \frac{T_{rotor}}{\frac{1}{2}\rho V_{ref}^2 A_{rotor}} \quad (3)$$

As the velocity is cubed in the power coefficient calculation, choosing a correct reference velocity was crucial for producing a good basis for result comparison. In a uniform flow, the position of the reference velocity measurement is insignificant, as the theoretical amount of energy hitting the turbine will be independent of position. However, the denominator in the  $C_p$  equation is strongly dependent on the reference height in wind shear measurements. To ensure that the position of the reference velocity was consistent with the actual center of energy in the rotor area, a three dimensional numerical integration of the energy profile was executed. The center of energy is at the height of the third root average wind speed, which is calculated in the following way:

$$U_{ref} = \sqrt[3]{\sum_{i=1}^{10} U_i^3 \frac{A_i}{A_{rotor}}} \quad (4)$$

The rotor was divided into 10 segments with area  $A_i$ , as the velocity,  $U_i$ , had been measured at 10 heights within the upper and lower limit of the rotor area. The calculation showed that the center of energy was 4 cm below hub height. This revealed that using the hub height velocity gave power coefficients approximately 2% lower than using the third root average of the velocity profile. To ensure the best possible comparability, the height of the reference velocity was therefore adjusted to 4 cm below hub height in all shear flow calculations, shown in Figure 4.

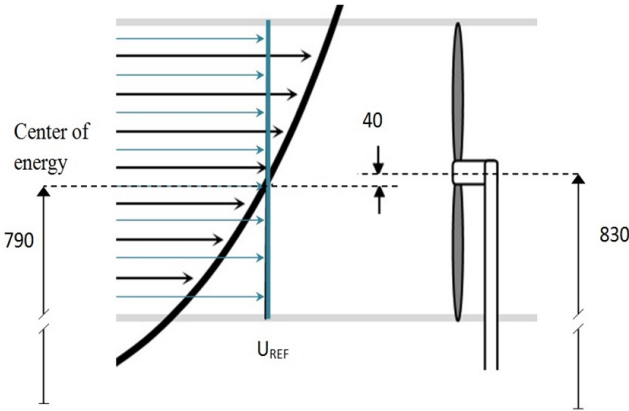


Figure 4: Velocity in reference height is slightly lower than the velocity in hub height, so that the "extra" energy above the reference height is equal to the missing energy below reference height. Dimensions are in millimetre.

### 3 RESULTS AND DISCUSSION

#### *Shear grid modification*

The grid design was modified several times, changing both the mesh sizes and the number of horizontal bars, which revealed that relatively large changes in mesh size often had only a small effect on the wind profile. However, a

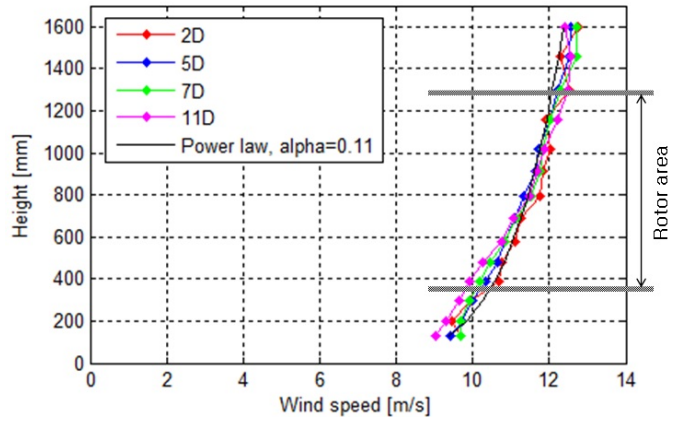


Figure 5: Wind profile measured 2, 5, 7 and 11 diameters downstream shear generating grid.

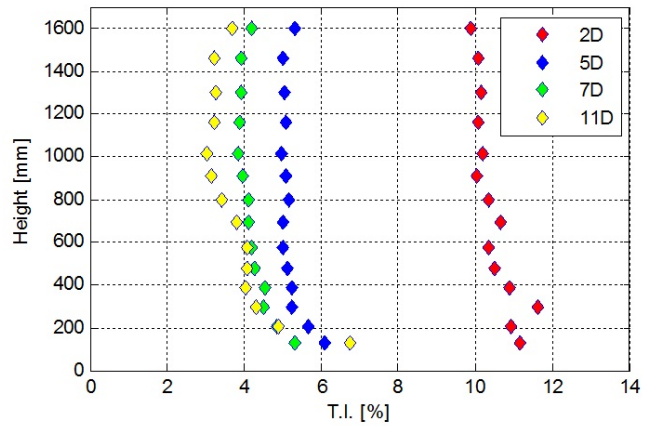


Figure 6: Turbulence intensity measured 2, 5, 7 and 11 diameters downstream shear generating grid.

small position modification of the lowest horizontal bar had a large effect on the entire wind profile. After carefully adjusting this bar, the wind profiles shown in Figure 5 were achieved. The vertical profiles were measured at the four turbine positions, 2, 5, 7 and 11 diameters downstream of the grid. The figure shows that the wind profiles are relatively consistent with a power law wind profile with a coefficient  $\alpha = 0.11$  and a wind speed of 11.5 m/s in hub height (830 mm). The wind profiles reveal a small increase in the wind shear gradient towards the end of the test section.

The turbulence intensities were measured with a single hot wire (see Figure 6). The turbulence intensity from the shear grid is about the same as from the quadratic grid at the 2D-position. 10-11 % is slightly higher than what is expected in typical offshore wind conditions. However, it decreases rapidly, and lies between 3 and 5 % in the three downstream positions. The turbulence levels slightly increase close to the tunnel floor, relative to the rest of the turbulence profile.



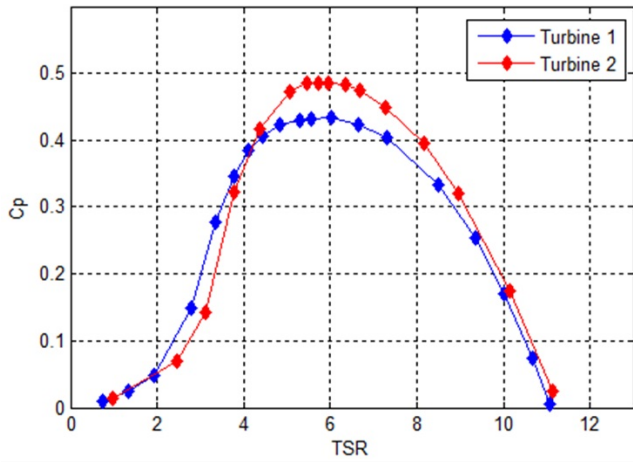


Figure 7: Cp of turbine 1 and 2 without interaction.

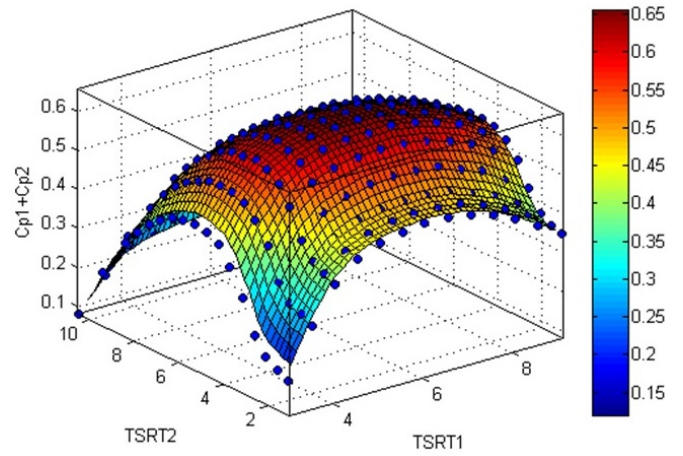


Figure 9: Cp T1 + Cp T2, with distance 5.3 diameters.

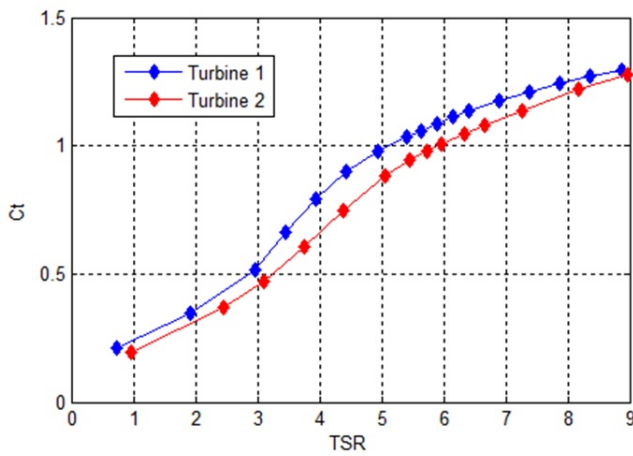


Figure 8: Ct of turbine 1 and 2 without interaction.

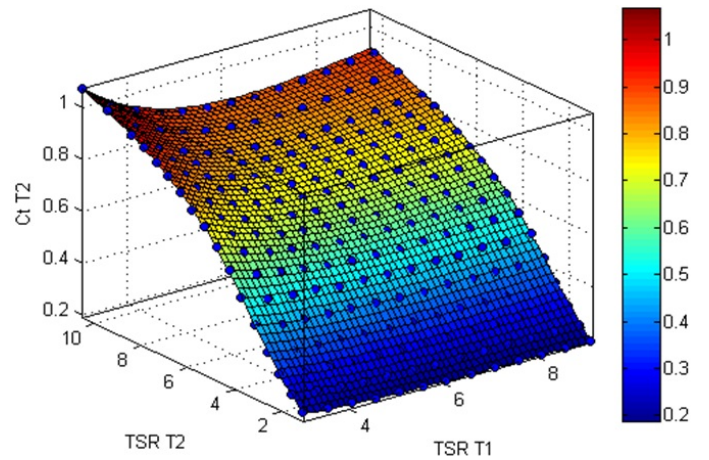


Figure 10: Ct for turbine 2 in the wake of turbine 1, with distance 5.3 diameters.

#### Single turbine efficiency and thrust

Figure 7 shows the efficiency of each turbine in an undisturbed air flow. Both turbines have optimal tip speed ratios of  $TSR=6$ , at which turbine 1 has a  $C_p$  of 0.43 and the  $C_p$  of turbine 2 is measured to be 0.49. The difference in maximum efficiency is due to the rotor blades being designed to fit the hub of turbine 2. The thrust coefficients (Figure 8) shows that turbine 1 has a higher drag than turbine 2.

#### Turbine interaction in a shear flow

Figure 9 shows a summation of the power coefficients of both turbines. The blue dots represent the points in which the  $C_p$  value has been measured, and the coloured surface is linearised between these points. This plot is based on the results from measurements with a turbine distance of 5.3 diameters, but the shape of the plot is relatively similar with turbine distances of 3.2 and 9 diameters. The total  $C_p$  is quite stable around the optimal tip speed ratios, and operating turbine 1 at a tip speed ratio within a  $TSR$  of  $6 \pm 1$  will not change the total  $C_p$  more than 2%.

Figure 10 shows the thrust coefficient of turbine 2 in the 5D measurement. As the thrust coefficient of turbine 1 is independent of the tip speed ratio of turbine 2 ( $TSR$  T2), it will stay as in Figure 8 in all measurements. However, the thrust coefficient of turbine 2 shows to be quite strongly affected by turbine 1. Standing behind an optimally operated turbine 1, the second turbine experiences a drag which is around 2/3 of what it experiences in an undisturbed flow. The thrust coefficient is lowest when turbine 1 runs at optimal rotational speed, since this is when turbine one extracts the most energy from the wind.

To further investigate the power and thrust coefficients in a shear flow, a selection of featured measurements are presented in Figure 11 and 12. The plots are based on measurements conducted at turbine 1 tip speed ratios ( $TSR$  T1) of 5, 6 and 7, and for all three turbine distances (3.2, 5.3 and 9.0 diameters). The results show a distinctively improved total efficiency at a large turbine distance. Focusing on a tip speed ratio of 6 for turbine 1 reveals an improvement of maximum total  $C_p$  from 0.66

with distance 5.3 diameters to 0.7 with distance 9.0 diameters. Since turbine 1 experiences the same wind conditions in all measurements, the improvement of total  $C_p$  is solely due to better wind conditions for turbine 2, meaning that the efficiency of turbine 2 has increased with over 20 %. The increase in  $C_p$  for turbine 2 from 3.2 to 5.3 diameters at the same tip speed ratios is 15 %. An investigation of how the tip speed ratio of turbine 1 affects the  $C_p$  of turbine 2 reveals that for all turbine distances, a turbine 1 TSR of 5 gives a higher total  $C_p$  than a turbine 1 TSR of 7. In the 9D measurement, this proved to be partly due to an increase in turbine 1  $C_p$ , but in the 3D and 5D measurements the  $C_p$  of turbine 1 was equal at the two different TSRs. This means that although turbine 1 extracts the same amount of energy, turbine 2 still experience more energy in the wind if turbine 1 operates at  $TSR=5$ . The increase in turbine 2  $C_p$  is 5 % at distance 5.3 diameters and 9 % at distance 3.2 diameters. One hypothesis is that this is a result of turbine 1 blocking the wind more effectively at higher tip speed ratios, but this would have to be further examined before making a conclusion. However, the shift of maximum power coefficient towards a lower optimal TSR for turbine 1 occurs in all turbine distances, and is also examined in Figure 14.

Figure 12 presents the measured thrust coefficient of turbine 2 as function of the turbine's tip speed ratio. The graph shows that the increase in  $C_t$  is steeper the larger the turbine distance is, i.e. with more energy in the wind. It also shows that the thrust is more dependent on the tip speed ratio of turbine 1 when there is a small distance between the two turbines. Operating turbine 1 at a TSR of 5 will lead to a slightly higher  $C_t$  on turbine 2 than operating it at a TSR of 7.

The torque and the thrust are measured in wind which is significantly decelerated by turbine 1. However, exactly how much the velocity has decelerated is not known, and the turbine 2 TSR therefore uses the free stream velocity of 11.5 m/s as reference. This leads to a displacement of the measured  $C_p$  and  $C_t$  values towards a TSR which is lower than the actual value, since  $TSR = \frac{2\pi\omega}{60U_{ref}}$ , where  $\omega$  is the rotational speed of the turbine. The difference between the wake velocity and the free stream reference velocity is highest when turbine 2 is positioned close to turbine 1, meaning that the plot from the 3D measurement has the largest displacement of tip speed ratio. Accordingly, the 9D plot is closest to its actual TSR position. This displacement effect is why the thrust coefficient in Figure 12 is measured to be larger in the 5D measurement than in the 9D measurement at low turbine 2 tip speed ratios.

*The effects of turbulence and shear on turbine performance*

In addition to investigating how rotational speed and turbine spacing affects the turbine performance in a shear

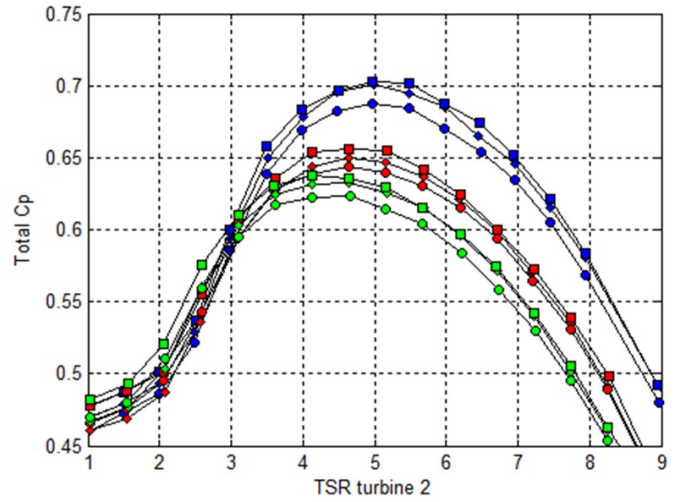


Figure 11: Total  $C_p$  measured at turbine 1 tip speed ratios of 5, 6 and 7.

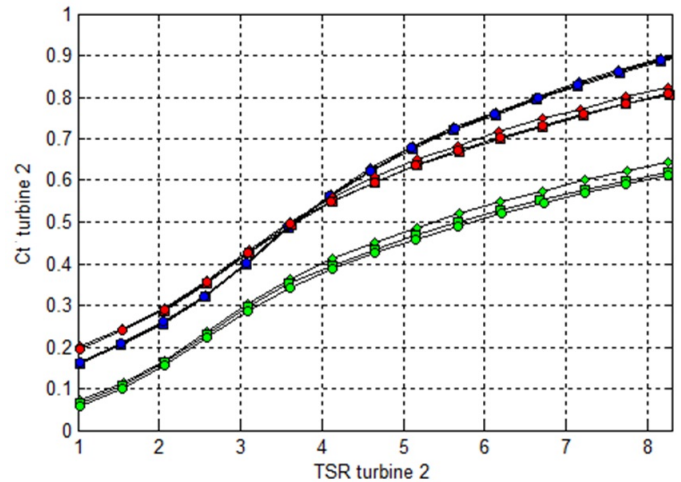
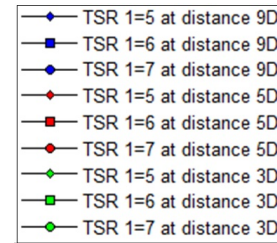


Figure 12:  $C_t$  for turbine 2 measured at turbine 1 tip speed ratios of 5, 6 and 7

flow, a comparison to similar measurement in flows with and without turbulence was conducted. Although measurements in a shear flow were conducted with turbine distances of 3.2, 5.3 and 9.0 diameters and turbulent/non-turbulent measurements were conducted with turbine distances of 2.8, 5.2 and 9.0 diameters, all are hereby referred to as 3D, 5D and 9D measurements, respectively. Turbine



1 did not show any significant changes in performance in the different flow characteristics, but turbine 2 was more affected. The power coefficients of turbine 2 with a distance of 5D to turbine 1 are presented in Figure 13. The figure shows that in an air flow with no turbulence or wind shear, the downstream turbine has a lower  $C_p$  when turbine 1 is operated optimally, compared to the turbulence and shear flows. As a flow without turbulence or shear will have a lower mixing of the air in the turbine wake, there will be less energy in the incoming flow to turbine 2.

To further investigate how adjusting the tip speed ratios of both turbines correlates with the wind farm performance, a colourmap showing the performance as function of TSR turbine 1 and TSR turbine 2 is presented in Figure 14. The colour expresses the relation between the measured total power coefficient (the sum of  $C_p$  1 and  $C_p$  2) and the maximum possible total  $C_p$  in an undisturbed flow. As temperature and atmospheric pressure can affect the maximum  $C_p$ , it was decided to use the maximum  $C_p$  of turbine 1 in the current measurement as reference for the maximum  $C_p$  of both turbines, instead of separately measured maximum  $C_p$ s. Hence, the maximum  $C_p$  is unique for every colourmap, yet only with very small variations.

The shift of the optimal tip speed ratio of turbine 2 (vertical axis) is strongly present in the 3D measurements. Although the area of the tip speed ratios producing the maximum power coefficient includes several TSR compositions, operating turbine 2 at a TSR of between 4 and 4.5 seems to be an optimal operation point in all flows. Increasing the turbine distance to 5 diameters slightly shifts the optimal tip speed ratio of turbine 2 towards  $TSR = 4.5$ . Operating in a flow with no turbulence or shear, however, turbine 2 still has an optimal TSR closer to 4. This tendency continues in measurements conducted with a

turbine distance of 9D. The optimal TSR for turbine 2 has increased to 5 for all flows. Changing the focus towards the tip speed ratio of turbine 1 (horizontal axis), the differences are smaller between the different flows and turbine distances. In both the shear flow and turbulence measurements, turbine 1 tip speed ratios between 5 and 6.5 all seem to be in an optimal operating area at all distances.

In Figure 15, the power coefficient of turbine 1, turbine 2 and the sum of these two are presented as functions of tip speed ratio for turbine 1. In each graph, only data from the optimal tip speed ratio for turbine 2 is plotted. Hence, the 3D plot shows results from  $TSR T2 = 4$ , the 5D plot shows results from  $TSR T2 = 4.5$  and the 9D plot shows results from  $TSR T2 = 5$ . Also in this figure, the results have been corrected with an individual factor, so that all measurements have a maximum turbine 1  $C_p$  of 0.45. Again, this is to eliminate any effect on the  $C_p$  results coming from variations in atmospheric pressure.

It is very clear that for all turbine distances, the  $C_p$  of turbine 2 is significantly lower in a non-turbulent flow. Compared to these results, the turbine 2  $C_p$  in a shear flow is 25 % higher with turbine distance 5D and a turbine 1 TSR of 6. The difference between power coefficient measurements in a turbulent flow compared to a turbulent shear flow is very small, except in the 3D measurement. Here, the  $C_p$  is slightly higher in the flow with wind shear. This effect could imply that the shear has a positive effect on the air mixing at this distance, but it is also very likely that this is simply a result of the turbine spacing being 0.4 diameter larger in the shear flow measurement. The effect is not visible at larger turbine distances, where the power coefficients are practically equal.

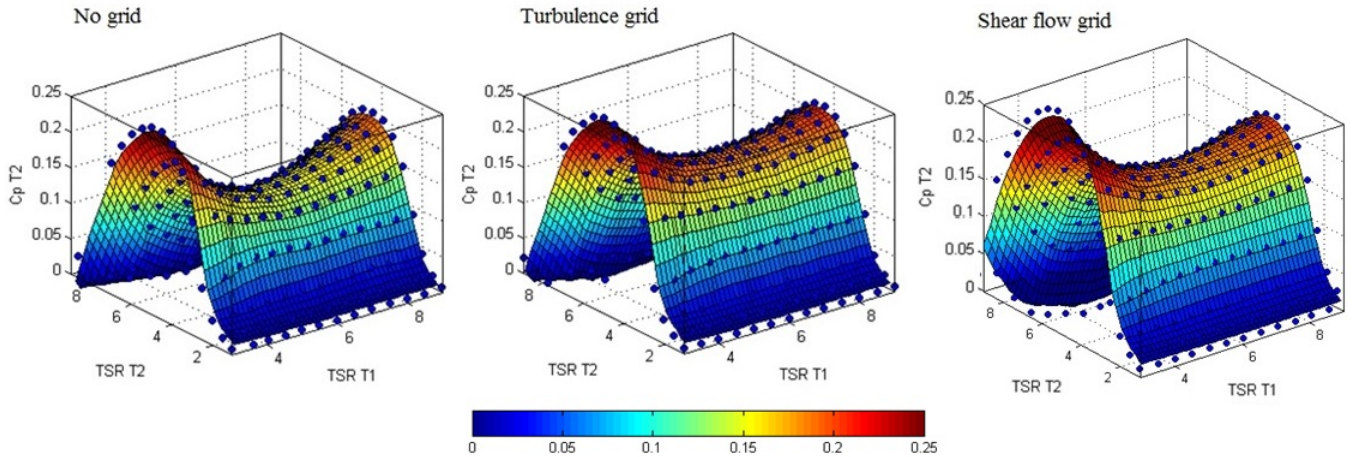


Figure 13: Comparison of turbine 2  $C_p$  without grid, with turbulence grid and with shear flow grid.

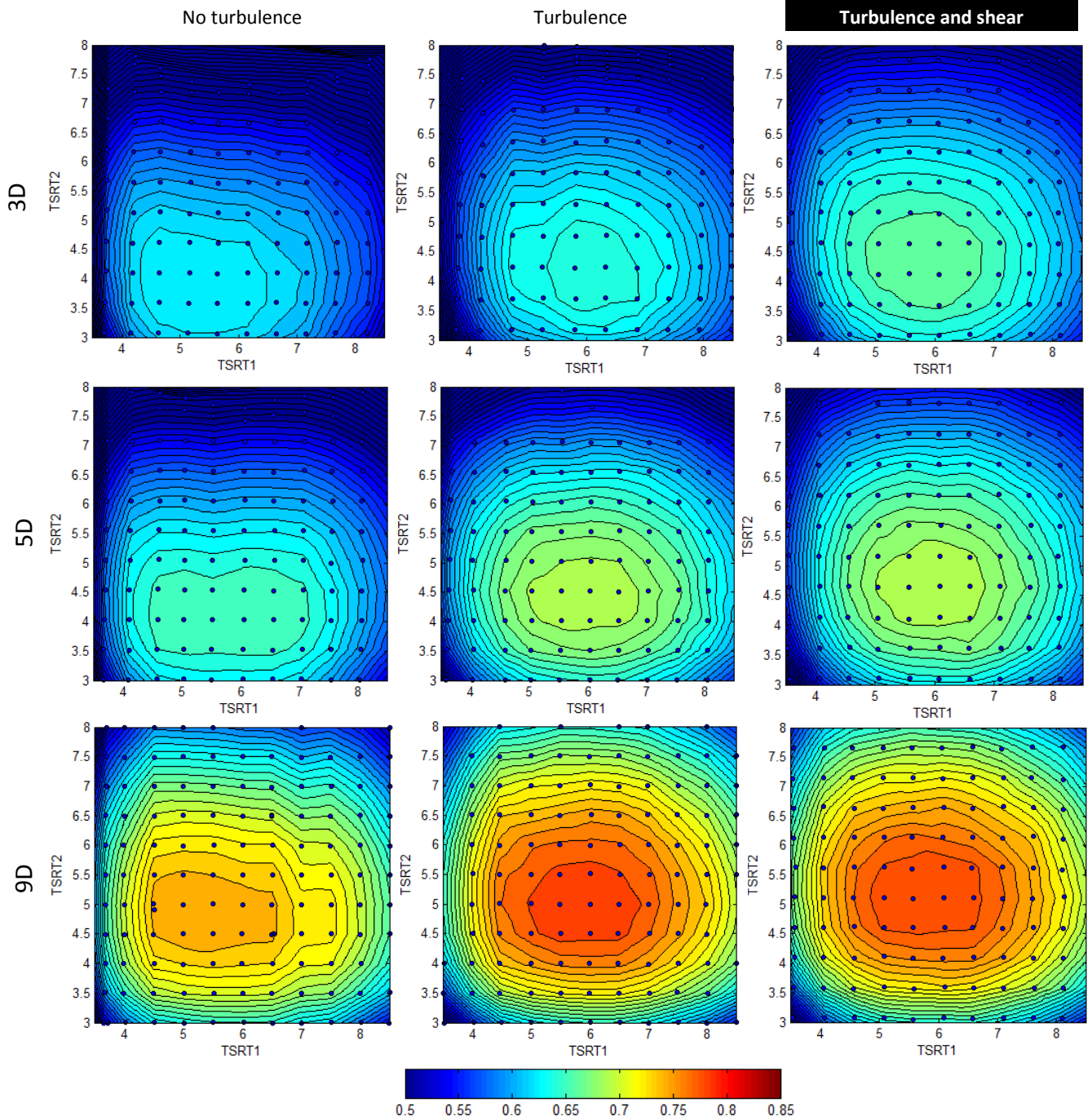


Figure 14: Colours representing the total  $C_p$  (sum of both turbines) of each measurement relative to the maximum possible total  $C_p$ .

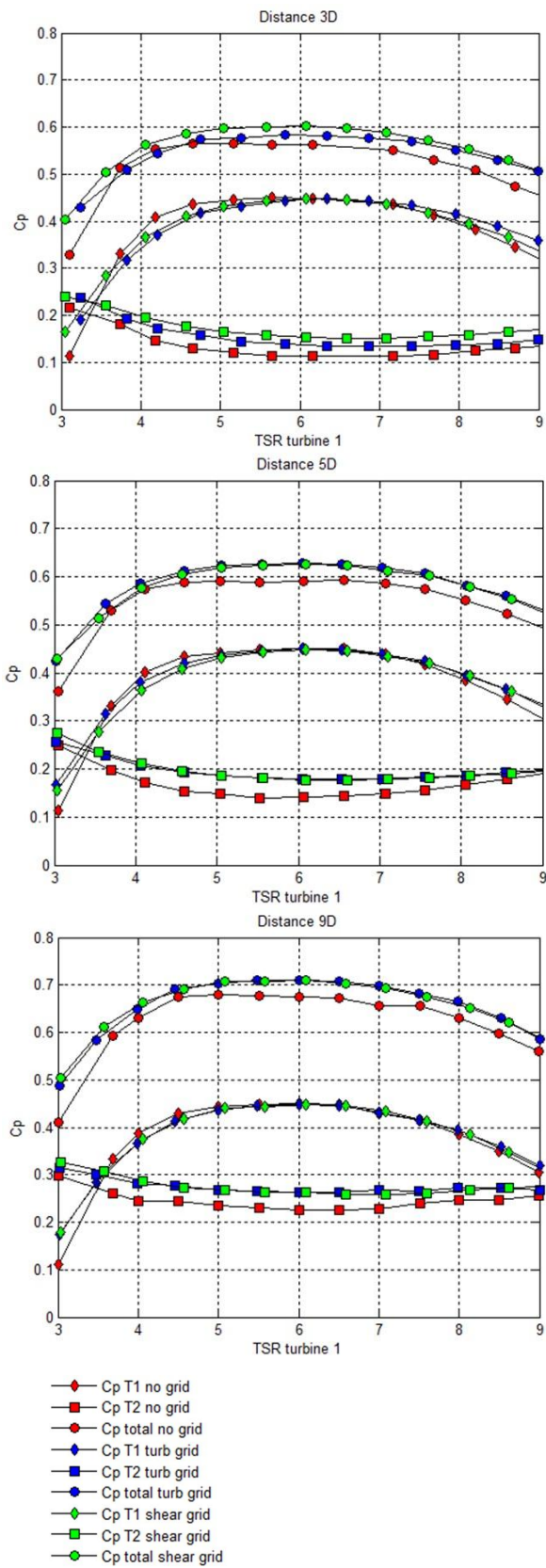


Figure 15: The separate and totalised turbine efficiencies measured at optimal tip speed ratio for turbine 2.

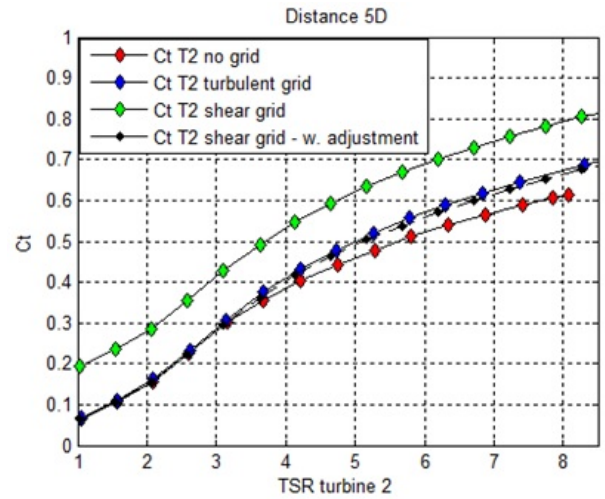


Figure 16: Thrust coefficients measured on turbine 2 at distance 5D and turbine 1 TSR of 6.

#### Comparison of thrust coefficient

Figure 16 shows the measured thrust coefficients of turbine 2, when turbine 1 operates at  $TSR = 6$  and there is a distance of 5 diameters between the turbines. The reason for the relatively large difference in thrust measured in a shear flow compared to the uniform flow has not been established, but several parameters affect the results to varying degrees. One influence is the shifting of the  $C_t$  curves from using the free stream velocity as a reference for the tip speed ratios. This creates uncertainties in the comparison of thrust in different flows. There is also a possibility of human errors in both the experimental procedures and the post-processing of experimental data. Assuming that the difference in  $C_t$  is simply caused by an incorrect offset reading would mean that the incorrect thrust measurement could be moved vertically dependent on the size of the misreading. Assuming that the two turbulent flows will produce the same thrust at a tip speed ratio of 0, a parallel adjustment of the shear flow thrust is added to the plot, shown as a black line. If these assumptions are correct, this may indicate that the difference in thrust caused by wind shear is almost non-existent.

## 4 CONCLUSION AND FURTHER WORK

This study investigated the effects of adjusting tip speed ratios and turbine distance on the wind farm efficiency in a shear flow. The results may be used as benchmark cases when searching for optimal design and operation of full scale wind farms, as well as comparison cases to computational simulation models. The results were also compared to model turbine performance measurements conducted in uniform flows with and without turbulence, to investigate the effects of wind shear and turbulence.

### *Shear flow measurement*

The turbine performance with turbine spacings of 3.2, 5.3 and 9.0 diameters were measured in a shear flow imitating offshore wind conditions with turbulence intensity variations between 3 % and 11 % and a power law exponent of 0.11. This resulted in maximum total power coefficients of 63 %, 66 % and 70 % with the different turbine distances, respectively. As this increase came almost exclusively from turbine 2, this turbine had an increase in  $C_p$  of 15 % and 20 % when adjusting the turbine distance from 3.2 to 5.3 and from 5.3 to 9.0 diameters, respectively.

Reducing the tip speed ratio of turbine 1 from  $TSR = 7$  to  $TSR = 5$  had no effect on the power coefficient of the upstream turbine at turbine distances of 5.3 and 3.2 diameters. Still, the power coefficient of the downstream turbine had an increase of 5 % and 9 %, respectively. This means that although turbine 1 extracts an equal amount of energy from the wind, turbine 2 still experience more energy if turbine 1 operates at a lower  $TSR$ . This effect was not present at the highest turbine distance of  $9D$ , and obviously decrease to insignificant levels at high turbine distances. However, this means that a small reduction of the tip speed ratio of upstream turbines may have a positive effect on the total energy production in a wind farm when downstream turbines experience wake losses, and also that the extent of this effect depends on the turbine distance.

Measuring the thrust on the downstream turbine proved to be strongly dependent on the turbine distance, and slightly dependent on the tip speed ratio of turbine 1 at turbine spacings of 3.2 and 5.3 diameters. Hence, the positive effect on the  $C_p$  of turbine 2 due to a reduced tip speed ratio of turbine 1 is followed by a negative effect of higher  $C_t$  on turbine 2.

### *Comparison measurements*

The comparison of measurements conducted in varying wind conditions revealed large improvements of turbine 2 efficiencies in a turbulent shear flow compared to a uniform flow without turbulence. This confirms the positive effects of effective air mixing behind an upstream turbine. The power coefficient of turbine 2 was for instance 25 % higher in the shear flow at optimal tip speed ratios and turbine distance  $5D$ . Comparing the measurement of a uniform turbulent flow with the shear flow did however not reveal any large differences. The only measurement resulting in a different  $C_p$  was the  $3D$  measurement, where the shear seemed to provide more energy to turbine 2 faster than the uniform turbulent flow. The difference in turbine 2  $C_p$  was about 9 % at optimal  $TSRs$  in this measurement, but may however come from the fact that the shear flow measurements had a turbine distance which was 0.4 diameter larger. In general, the effects from adjusting tip speed ratio of turbine 1 were all most present in measurements where the air mixing between the turbines is smallest, i.e. at small

turbine distances and without wind turbulence.

### *Further work*

For further studies in the NTNU wind tunnel using the shear generating grid, a thorough examination of the three dimensional wind field would help understanding the characteristics of the flow, and possibly reduce the uncertainty when choosing a reference velocity for performance calculations. Another research possibility using shear generating grids is studying in what extent the wind shear creates an oblique load on the rotor blades, leading to a pitch momentum on the turbine. This, and examining how a turbine standing partially in the wake of an upstream turbine experiences a yaw momentum from the uneven horizontal energy distribution, could increase the knowledge about wind turbine wear and fatigue.

To examine the wake losses relative to the turbine distance, more model turbine measurements should be conducted at typical full scale turbine distances, such as 7 and 8 diameters. Such measurements would contribute in the challenge of finding the optimal turbine distance, when comparing wind farm production with costs related to area and infrastructure. Also a further investigation of the effect on turbine 2  $C_p$  when reducing the tip speed ratio of the upstream turbine could be conducted, helping to understand this effect in detail.

## REFERENCES

- [1] Rebecca Barthelmie, Gunner Larsen, Sara Pryor, Hans Jørgensen, Hans Bergström, Wolfgang Schlez, Kostas Rados, Bernhard Lange, Per Vølund, Søren Neckelmann, et al. Endow (efficient development of offshore wind farms): modelling wake and boundary layer interactions. *Wind Energy*, 7(3):225–245, 2004.
- [2] RJ Barthelmie, GC Larsen, ST Frandsen, L Folkerts, K Rados, SC Pryor, B Lange, and G Schepers. Comparison of wake model simulations with offshore wind turbine wake profiles measured by sodar. *Journal of atmospheric and oceanic technology*, 23(7):888–901, 2006.
- [3] International Electrotechnical Commission et al. Iec 61400-1. *Wind Turbines Part 1: Design Requirements*, 2005.
- [4] International Electrotechnical Commission et al. Iec 61400-3. *Wind Turbines Part 3: Design Requirements for Offshore Wind Turbines*, 2009.
- [5] PA Davidson and P-Å Krogstad. On the deficiency of even-order structure functions as inertial-range diagnostics. *Journal of Fluid Mechanics*, 602:287–302, 2008.
- [6] Benedikt Ernst and Jörg R Seume. Investigation of site-specific wind field parameters and their effect on

- loads of offshore wind turbines. *Energies*, 5(10):3835–3855, 2012.
- [7] SA Hsu, Eric A Meindl, and David B Gilhousen. Determining the power-law wind-profile exponent under near-neutral stability conditions at sea. *Journal of Applied Meteorology*, 33(6):757–765, 1994.
- [8] P-Å Krogstad and JA Lund. An experimental and numerical study of the performance of a model turbine. *Wind Energy*, 15(3):443–457, 2012.
- [9] Per-Åge Krogstad and Pål Egil Eriksen. blind test calculations of the performance and wake development for a model wind turbine. *Renewable Energy*, 50:325–333, 2013.
- [10] Per-Åge Krogstad, Lars Sætran, and Muiyiwa Samuel Adaramola. blind test 3 calculations of the performance and wake development behind two in-line and offset model wind turbines. *Journal of Fluids and Structures*, 2014.
- [11] Søren Krohn, Poul Erik Morthorst, Shimon Awerbuch, et al. *The economics of wind energy*. European Wind Energy Association Brussels, 2009.
- [12] Fabio Pierella, Per-Åge Krogstad, and Lars Sætran. Blind test 2 calculations for two in-line model wind turbines where the downstream turbine operates at various rotational speeds. *Renewable Energy*, 2014.
- [13] Y Tamura, Y Iwatani, K Hibi, K Suda, O Nakamura, T Maruyama, and R Ishibashi. Profiles of mean wind speeds and vertical turbulence intensities measured at seashore and two inland sites using doppler sodars. *Journal of wind engineering and industrial aerodynamics*, 95(6):411–427, 2007.
- [14] LJ Vermeer, Jens Nørkær Sørensen, and A Crespo. Wind turbine wake aerodynamics. *Progress in aerospace sciences*, 39(6):467–510, 2003.